Electronic Supplementary Information

A Hydrophobic Semiconducting Metal-organic Framework Assembled from Silver Chalcogenide Wires

Jia-Yin Wang,[‡,a,b] Wen-Hua Li,[‡,c] Zhong Wei,[b] Chong Zhang,[b] Ya-Hui Li,[b]

Xi-Yan Dong,[*a,b] Gang Xu,[c] and Shuang-Quan Zang[*b]

[a]*College of Chemistry and Chemical Engineering, Henan Polytechnic University, Jiaozuo 454000, China.*
[b]*College of Chemistry and Molecular Engineering, Zhengzhou University, Zhengzhou 450001, China*
[c]*State Key Laboratory of Structural Chemistry, Key Laboratory of Design and Assembly of Functional Nanostructures, Fujian Provincial Key Laboratory of Nanomaterials, Fujian Institute of Research on the Structure of Matter, Chinese Academy of Sciences (CAS) 155 Yangqiao Road West, Fuzhou, Fujian 350002, P.R. China*

*E-mail: dongxiyan0720@hpu.edu.cn

zangsqzg@zzu.edu.cn

[‡]These authors contributed equally to this work.

Materials and Methods

Materials and reagents

All reagents and solvents used were of commercially available reagent grade and were used without any additional purification.

Characterization

The elemental analyses (C, H, S contents) were determined on a Perkin-Elmer 240 elemental analyzer. Thermogravimetric (TG) analyses were performed on a SDT 2960 thermal analyzer from room temperature to 400 ^{o}C at a heating rate of 10 ^{o}C/min under nitrogen atmosphere. PXRD patterns of the compounds were collected at room temperature in air on a X'Pert PRO diffractometer (Cu-Kα). The adsorption isotherm of N_2 at 77 K was measured by using a BEL-max physisorption analyzer after the elimination of guest molecules by evacuation at room temperature for 24 h. ^{1}H NMR spectra were recorded on a Bruker DRX spectrometer operating at 400 MHz in DMSO-d6. 300 mg complex **AgS-L** MOF were weighed and grinded. The pellets of AgS-L MOFs were formed at a pressure of $\approx$1 GPa. Contact angle (CA) were recorded on a SDC-200 contact angle meter at room temperature (water droplet volume = 3 μL). The vapor adsorption isotherms of H_2O were measured at room temperature by a gravimetric method using a 3H-2000PWz adsorption instrument. Scanning electron microscope (SEM) images and energy dispersive spectrometer (EDS) mapping images were acquired using a Zeiss Sigma 500 emission scanning electron microscope with an accelerating voltage of 2**–**10 kV for SEM images and 20 kV for EDS mapping images.

Single-crystal X-ray diffraction (SCXRD) measurements and details for structure determination

SCXRD measurements were performed on a Rigaku XtaLAB Pro diffractometer with Cu-Kα radiation (λ =1.54184 Å) at 200 K for **AgS-L**. Data collection and reduction were performed using the program CrysAlisPro.[1] The structures were solved with intrinsic phasing methods (*SHELXT-2015*)[2] and refined by full-matrix least squares on F^2 using *OLEX2*, which utilizes the *SHELXL-2015* module.[3] Intrinsic disorder occurred, although all X-ray intensity data displayed reasonably good quality as reflected by their low R_{int} (0.082) and R_{sigma} (0.096) values. Refinement of the solvent peaks failed because the solvent molecules are highly disordered. The imposed restraints in least-

squares refinement of each structure were commented in the corresponding CIF files. Thus, only a general description of the structural refinement strategy is presented here. All non-hydrogen atoms were refined anisotropically, and the hydrogen atoms were included on idealized positions. The crystal structures are visualized by DIAMOND 3.2.[4] The detailed information of the crystal data, data collection and refinement results for all compounds are summarized in Table S2. The fraction of the void space was calculated from the X-ray structural data of **AgS-L** by PLATON.

Luminescence decay measurements

Solid UV−visible spectrum was obtained in the 200−800 nm range on a JASCOUVIDEC-660 spectrophotometer. Luminescence measurements were carried out using a HORIBA FluoroLog-3 fluorescence spectrometer. Variable-temperature steady-state emission spectra of solid-state **AgS-L** were performed using an East Changing TC202 temperature controller after each sample was evacuated for 30 min using a VALUE VRD-16 vacuum pump.

Electrical Conductivity Measurement

The single-crystal electrodes were made using SPI conductive silver paint (SPI 05002-AB) by placing the crystal between two electrodes. The silver electrodes are connected with gold wires (diameter is 50 micrometers). The temperature-dependent I-V curve measurements for the single crystal of **AgS-L** with a direct current two terminal method were on KEITHLEY4200 with an oven. Each measurement was performed on several independent single crystals of **AgS-L**. The length of the crystals is about 300~500 μm.

Preparation of AgS-L

Bu^{t}SAg (0.02 g, 0.1 mmol) and CF_3COOAg (0.022 g, 0.1 mmol) were added into a mixed acetone / acetonitrile (CH_3CN) (3:2, 5.0 mL) solution. Subsequently, phenylphosphonic acid ($PhPO_3H_2$, 0.02 g, 0.13 mmol) and the CH_3CN solution of **H_2L** (0.01 g, 0.04 mmol) were sequentially added under rapidly stirring over 5 min. The resulting clear solution was then placed in a dark environment at room temperature for 1 day. Colorless acicular crystals were rinsed with CH_3CN, filtered and dried in air for 2 hours to obtain **AgS-L** in 13 % yield based on **H_2L**. Elemental analysis calcd. (%) for evacuated **AgS-L** ($C_{24}H_{36}Ag_6F_4O_4S_4$): C, 23.25; H, 2.93; S, 10.34. found: C, 23.57; H, 2.77; S, 9.77.

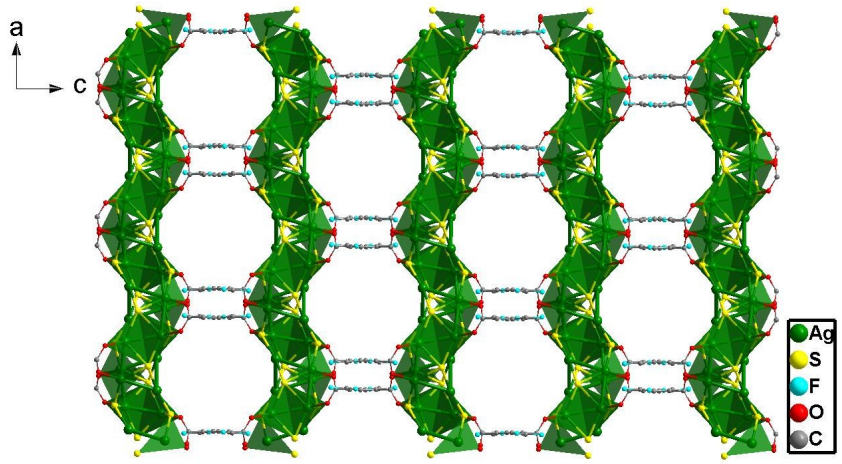

Fig. S1 Perspective drawings of the 3D structure of **AgS-L** viewed along the crystallographic *b*-axis. –^{t}Bu and H atoms are omitted for clarity.

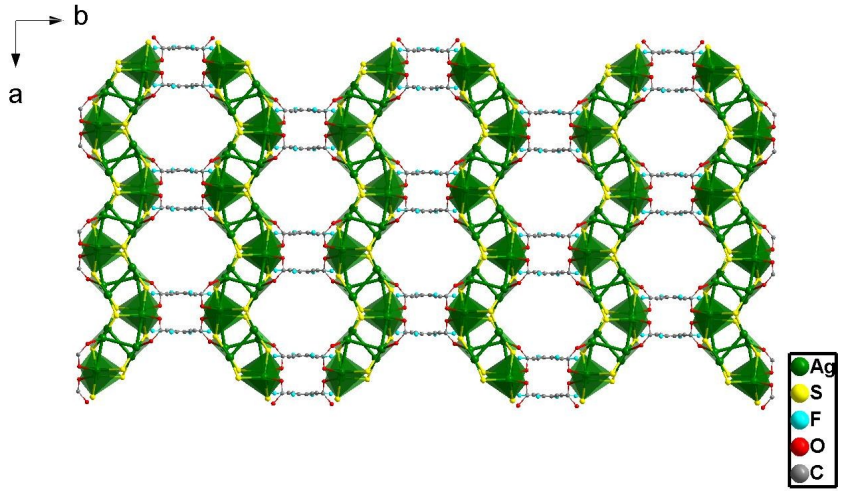

Fig. S2 Perspective drawings of the 3D structure of **AgS-L** viewed along the crystallographic *c*-axis. –^{t}Bu and H atoms are omitted for clarity.

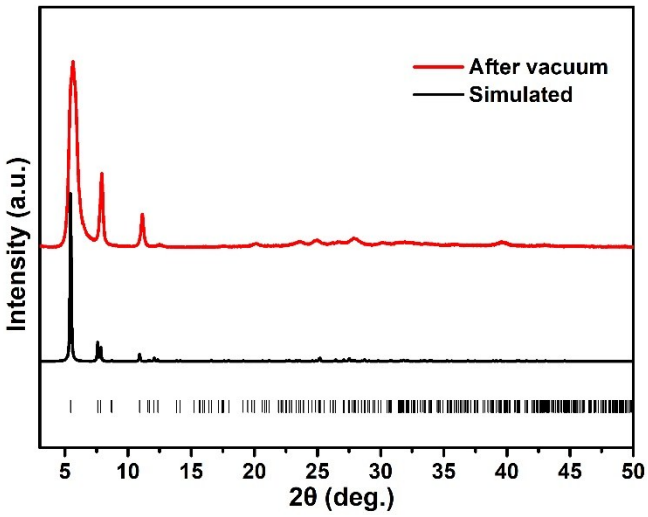

Fig. S3 PXRD patterns of **AgS-L** samples after vacuum treatment and the simulated one.

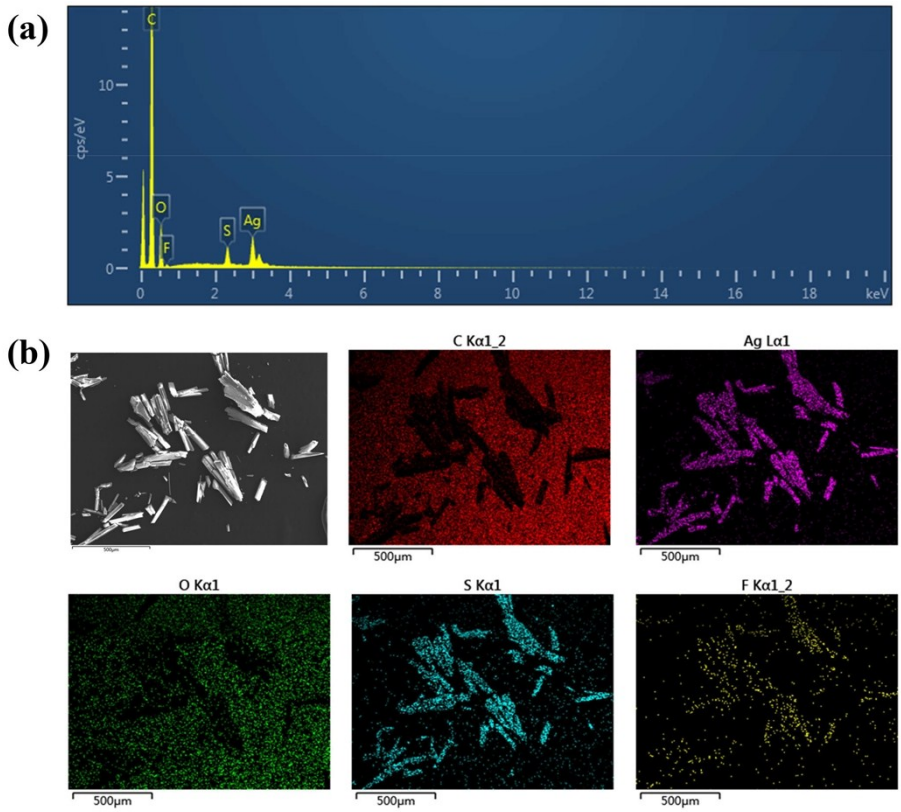

Fig. S4 (a) Energy Dispersive Spectrometer (EDS) analysis; (b) Elemental mapping images of evacuated **AgS-L**.

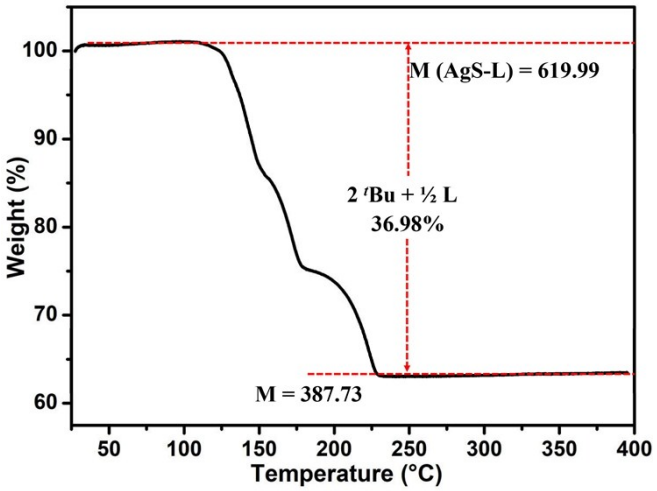

Fig. S5 Thermogravimetric analysis of **AgS-L** under N_2 atmosphere.

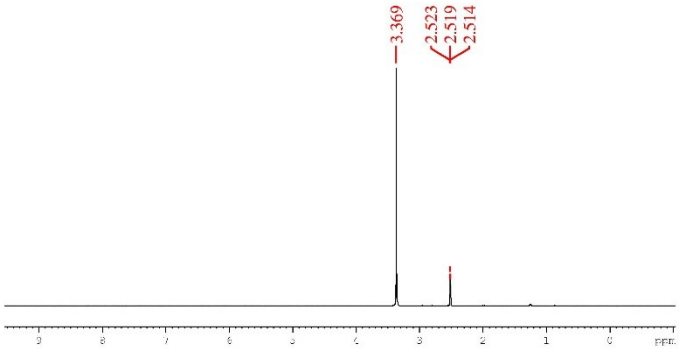

Fig. S6 ^{1}H-NMR (DMSO-d6, 400 MHz) specturm of **AgS-L**.

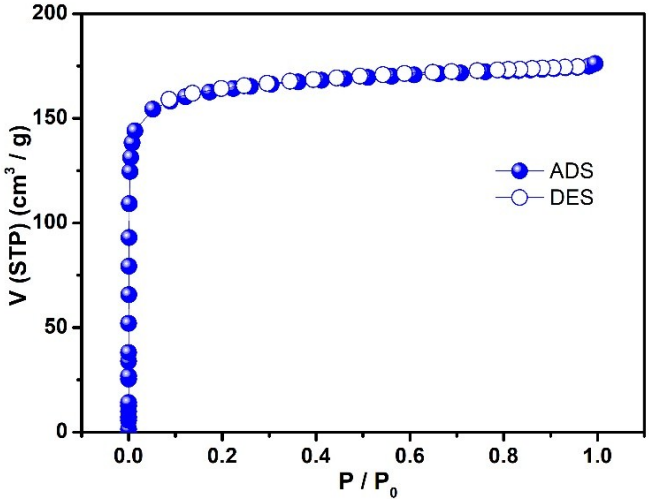

Fig. S7 N_2 adsorption (closed symbols) and desorption (open symbols) isotherms at 77 K of **AgS-L**.

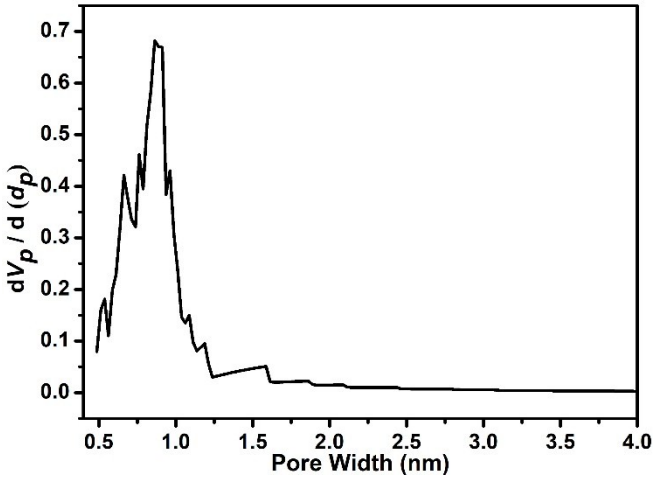

Fig. S8 The H-K micropore size distribution analysis of **AgS-L**.

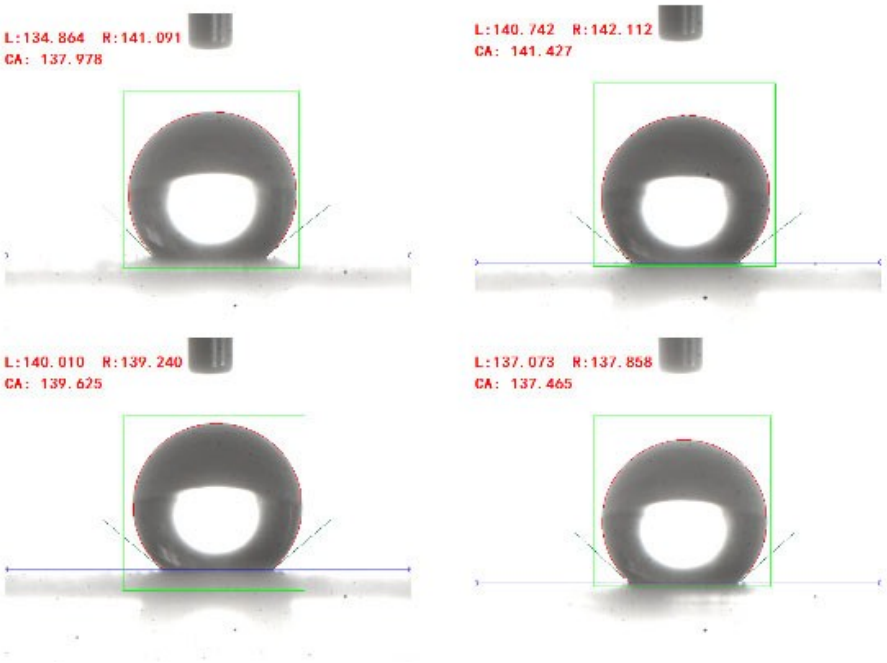

Fig. S9 Contact angle patterns for **AgS-L** at room temperature (water droplet volume = 3 μL).

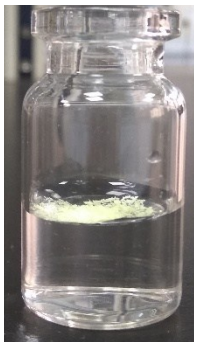

Fig. S10 Digital photographs of **AgS-L** floating on the water surface exhibits hydrophobic behavior.

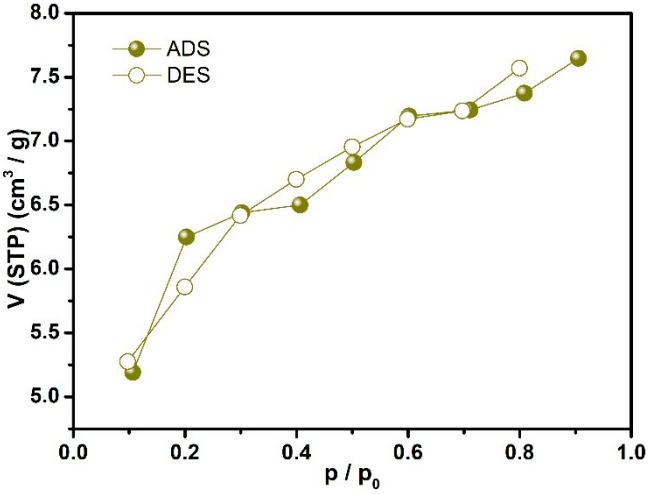

Fig. S11 H_2O adsorption (closed symbols) and desorption (open symbols) isotherms of **AgS-L** at 298 K.

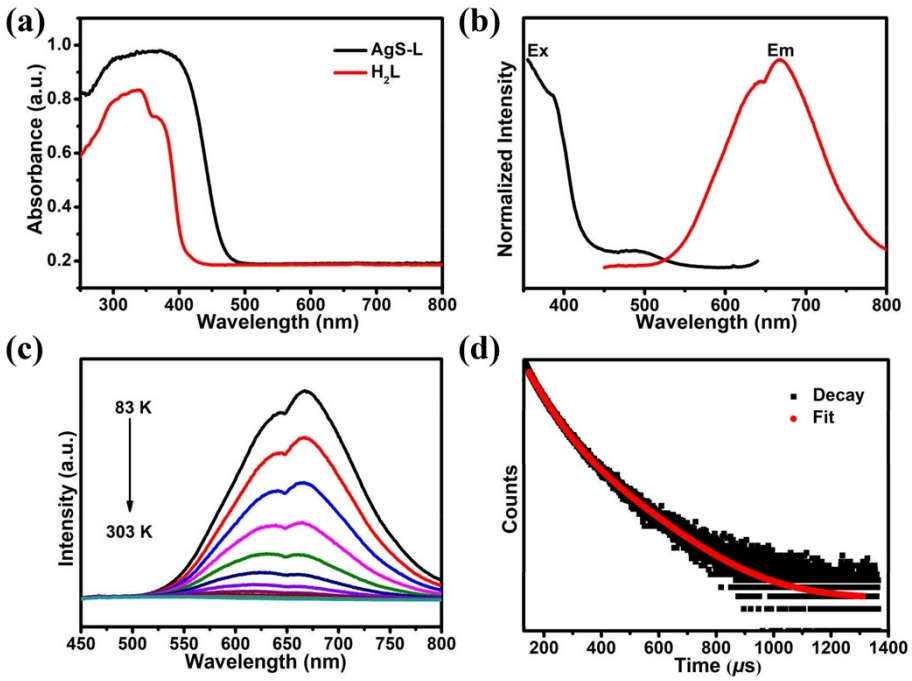

Fig. S12 (a) UV-Vis diffuse reflectance spectrum of **H_2L** and **AgS-L** at room-temperature. (b) Luminescence spectrum of **AgS-L** at 83 K. (c) Variable-temperature emission spectra of **AgS-L** (excited at 386 nm) from 83 K to 303 K. (d) Luminescence decays at 668 nm of **AgS-L** (355 nm SpectraLED as the excitation light).

AgS-L presents temperature-dependent luminescence under 365 UV irradiation. Under 386 nm UV light irradiation, the solid-state emission spectrum of **AgS-L** at 83 K displays an emission band centered at 668 nm (Fig. S12b). To quantify this observation, the solid-state emission spectra of **AgS-L** were recorded at varied temperatures. It barely emitted luminescence at ambient temperature which turned more and more brightly with the decrease of temperature (Fig. S12c). The emission of **AgS-L** could be tentatively assigned to ligand-to-metal-metal charge transfer (LMMCT; S→Ag) character mixed with metal-centered (ds/dp) states.[5] In addition, the luminescence transient decay at 668 nm with an observed lifetime of 64.23 μs at 83 K (Fig. S12d) was tentatively assigned to triplet states in the Ag-S chain nodes.[6]

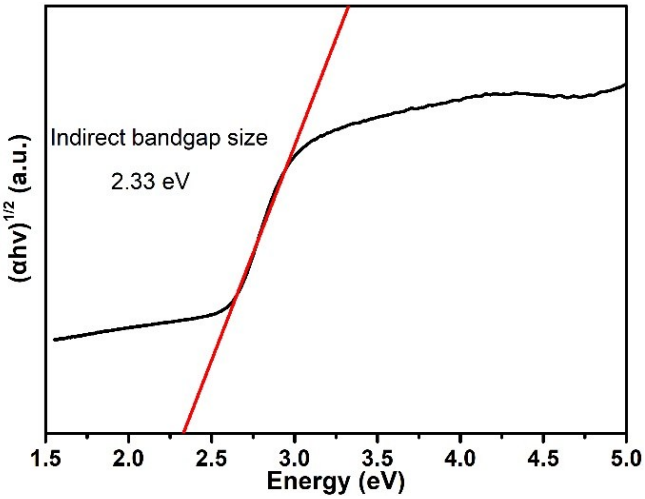

Fig. S13 Tauc plot displaying the band gap of **AgS-L**.

The bandgap for **AgS-L** MOF was calculated by means of the Tauc plot method and the equation for which is given as

$$(\alpha hv)^{1/2} = A(hv - E_g)$$

where α is the extinction coefficient, h is the Planck's constant (J.s), v is the light frequency (s^{-1}), A is the absorption constant and E_g is the band gap (eV). The indirect bandgap for the **AgS-L** MOF was estimated to be 2.33 eV.

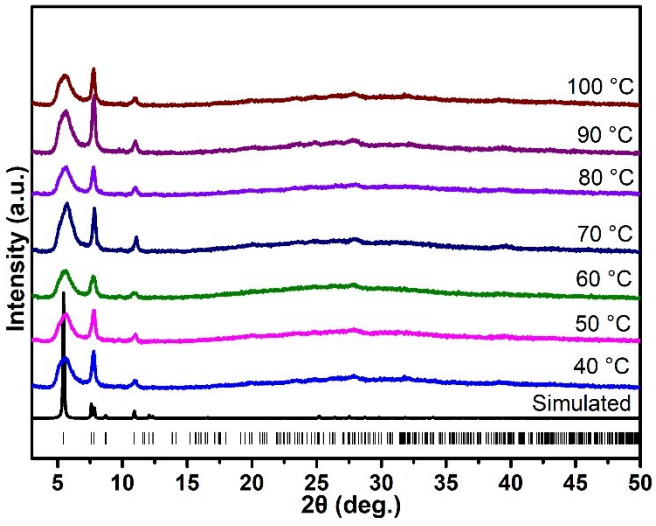

Fig. S14 PXRD patterns of **AgS-L** after annealing at different temperatures.

Table S1. The conducting properties of the reported atomically-precise Metal-S structures and **AgS-L** in this work.

Complex	Dimension	Interactions	Electrical Conductivity (S cm^{-1})	Activation Energy (eV)	Ref[7-14]
$\{[Ag_6(S^tBu)_4(L)]\cdot guest\}_n$	**3D**	**Ag-S**	**1.01×10^{-8}**	**0.35**	***(This Work)***
$\{[Cu_2(6\text{-}Hmna)(6\text{-}mn)]\cdot NH_4\}_n$	2D	Cu-S	10.96	6×10^{-3}	*Nat. Commun.* ***2019****, 10, 1721.*
$[In_{34}S_{54}]^{6-}$	3D	In-S	3×10^{-9}	0.34	*J. Am. Chem. Soc.* ***2018****, 140, 11189-11192.*
1ADCu	1D	Cu-S	1×10^{-4}	–	*Nat. Mater.* ***2017****, 16, 349-355.*
$[(CrO_4)_5@Ag_{40}(S^iBu)_{27}(CF_3COO)_3]_n$	1D	Ag···Ag Ag-S	3.99×10^{-8}	1.91	*Nanoscale* ***2017****, 9, 5305-5314.*
$[(CrO_4)_2@Ag_{41}(S^iBu)_{30}(NO_3)_3(CN)_4]_n$	3D	Ag···Ag Ag-S	2.59×10^{-9}	1.99	*Nanoscale* ***2017****, 9, 5305-5314.*
$Fe_2(DSBDC)(DMF)_2\cdot x(DMF)$	3D	Fe-S	3.9×10^{-6}	0.27	*J. Am. Chem. Soc.* ***2015****, 137, 6164-6167.*
$Mn_2(DSBDC)(DMF)_2\cdot x(DMF)$	3D	Mn -S	2.5×10^{-12}	0.81	*J. Am. Chem. Soc.* ***2015****, 137, 6164-6167.*
$[Pb_3(C_6S_6)]_n$	3D	Pb-S	2×10^{-6}	0.37	*J. Am. Chem. Soc.* ***2008****, 130, 14-15.*
$[Ag_{0.5}(btp)_{0.5}(ClO_4)_{0.5}]$	1D	Ag···π π-π	1.32	–	*Angew. Chem. Int. Ed.* ***2000****, 39, 4555-4557.*
$[\{Ag(C_5H_4NS)_n\}]$	2D	Ag-S	2.04×10^{-5}	–	*Angew. Chem. Int. Ed.* ***2000****, 39, 2911-2914.*

Table S2. Crystal data and structure refinements of **AgS-L**.

	AgS-L
CCDC number	1942249
Empirical formula	$C_{12}H_{18}Ag_3F_2O_2S_2$
Formula weight	619.99
Temperature / K	200.00(10)
Crystal system	orthorhombic
Space group	$I2_12_12_1$
a / Å	11.3195(7)
b / Å	22.5808(11)
c / Å	23.2576(14)
α / °	90
β / °	90
γ / °	90
Volume / Å^3	5944.7(6)
Z	8
ρ_{calc} g / cm^3	1.385
μ / mm^{-1}	17.122
F(000)	2376.0
Crystal size / mm^3	0.3 × 0.05 × 0.04
Radiation	Cu Kα (λ = 1.54184)
2θ range for data collection / °	5.454 to 149.63
Index ranges	$-10 \le h \le 13$, $-28 \le k \le 27$, $-27 \le l \le 28$
Reflections collected	9730
Independent reflections	5168 [R_{int} = 0.0818, R_{sigma} = 0.0961]
Data / restraints / parameters	5168 / 106 / 197
Goodness-of-fit on F^2	1.109
Final *R* indexes [I >= 2σ (I)]	R_1 = 0.1206, wR_2 = 0.3083
Final *R* indexes [all data]	R_1 = 0.1409, wR_2 = 0.3235
Largest diff. peak/hole / e Å^{-3}	3.01 / −1.61
Flack parameter	0.24(6)
Removed electron density	818.3

$R_1 = \sum||F_o|-|F_c||/\sum|F_o|$. $wR_2 = [\sum w(F_o^2 - F_c^2)^2/\sum w(F_o^2)^2]^{1/2}$

Table S3. Selected Bond Distances for Complex **AgS-L**.

Atom–Atom	Bond length	Atom–Atom	Bond length
Ag1–Ag1[1]	3.364(5)	Ag2–S1[1]	2.682(8)
Ag1–Ag3[2]	3.027(3)	Ag2–S2	2.519(7)
Ag1–S1	2.407(7)	Ag2–O1	2.26(2)
Ag1–S2	2.361(7)	Ag3–Ag3[5]	3.244(5)
Ag2–Ag2[3]	2.911(5)	Ag3–S1[4]	2.555(8)
Ag2–Ag3	3.047(4)	Ag3–S2[5]	2.475(7)
Ag2–S1[4]	2.720(7)	Ag3–O2	2.29(2)

Symmetry codes: [1]1-*X*, 3/2-*Y*, +*Z*; [2]1/2+*X*, 3/2-*Y*, 1-*Z*; [3]1/2-*X*, +*Y*, 1-*Z*; [4]-1/2+*X*, 3/2-*Y*, 1-*Z*; [5]-*X*, 3/2-*Y*, +*Z*.

References

[1] L. J. Bourhis, O. V. Dolomanov, R. J. Gildea, J. A. Howard, H. Puschmann, Acta Crystallogr. Sect. A **2015**, 71, 59–75.

[2] G. M. Sheldrick, Acta Cryst. A **2015**, *71*, 3-8.

[3] O. V. Dolomanov, L. J. Bourhis, R. J. Gildea, J. A. K. Howard, H. Puschmann, J. Appl. Cryst. **2009**, *42*, 339-341

[4] Brandenburg, K. *Diamond*, **2010**.

[5] a) R.-W. Huang, X.-Y. Dong, B.-J. Yan, X.-S. Du, D.-H. Wei, S.-Q. Zang, and T. C. W. Mak, *Angew. Chem. Int. Ed.* **2018**, *57*, 8560-8566; b) Z. Wang, H.-F. Su, C.-H. Tung, D. Sun, L.-S. Zheng, *Nat. Commun.* **2018**, *9*, 4407-4414; c) Z. Wang, H.-T. Sun, M. Kurmoo, Q.-Y. Liu, G.-L. Zhuang, Q.-Q. Zhao, X.-P. Wang, C.-H. Tung, D. Sun, *Chem. Sci.* **2019**, *10*, 4862-4867.

[6] J.-W. Liu, Z. Wang, Y.-M. Chai, M. Kurmoo, Q.-Q. Zhao, X.-P. Wang, C.-H. Tung, D. Sun, *Angew. Chem. Int. Ed.* **2019**, *58*, 6276-6279.

[7] A. Pathak, J. W. Shen, M. Usman, L. F. Wei, S. Mendiratta, Y. S. Chang, B. Sainbileg, C. M. Ngue, R. S. Chen, M. Hayashi, T. T. Luo, F. R. Chen, K. H. Chen, T. W. Tseng, L. C. Chen and K. L. Lu, *Nat. Commun.* **2019**, *10*, 1721.

[8] H. Yang, J. Zhang, M. Luo, W. Wang, H. Lin, Y. Li, D. Li, P. Feng and T. Wu, *J. Am. Chem. Soc.* **2018**, *140*, 11189-11192.

[9] H. Yan, J. N. Hohman, F. H. Li, C. Jia, D. Solis-Ibarra, B. Wu, J. E. Dahl, R. M. Carlson, B. A. Tkachenko, A. A. Fokin, P. R. Schreiner, A. Vailionis, T. R. Kim, T. P. Devereaux, Z. X. Shen and N. A. Melosh, *Nat. Mater.* **2017**, *16*, 349-355.

[10] X. Y. Li, H. F. Su, M. Kurmoo, C. H. Tung, D. Sun and L. S. Zheng, *Nanoscale* **2017**, *9*, 5305-5314.

[11] L. Sun, C. H. Hendon, M. A. Minier, A. Walsh and M. Dinca, *J. Am. Chem. Soc.* **2015**, *137*, 6164-6167.

[12] D. L. Turner, T. P. Vaid, P. W. Stephens, K. H. Stone, A. G. DiPasquale and A. L. Rheingold, *J. Am. Chem. Soc.* **2008**, *130*, 14-15.

[13] M. Munakata, G. L. Ning, Y. Suenaga, T. Kuroda-Sowa, M. Maekawa and T. Ohta, *Angew. Chem. Int. Ed.* **2000**, *39*, 4555-4557.

[14] W. Su, M. Hong, J. Weng, R. Cao and S. Lu, *Angew. Chem. Int. Ed.* **2000**, *39*, 2911-2914.